SUPPLEMENTARY METHODS AND FIGURES

METHODS

Patients and relatives. aHUS is a rare life threatening renal disease characterized by thrombocytopenia, Coombs test negative microangiopathic hemolytic anemia and acute renal failure triggered by vascular endothelial damage. aHUS affects primarily children and young adults. In contrast, AMD is a common eye condition among elderly people characterized by thickening of the Bruch's membrane and progressive formation of subretinal extracellular deposits (drusen) in the "dry" form which can progress to a more severe exudative "wet" form characterized by choroidal neovascularization and retinal edema. AMD presents similarities with subtypes of C3G, a heterogeneous group of rare glomerulopathies leading to renal failure characterized by massive deposition of C3 derivatives along the glomerular basement membrane (1-3).

Our study included 13 aHUS and 1 C3G patients of Spanish and Italian origins and 13 healthy relatives. All of them carry the FH R1210C mutation in heterozygosis. aHUS was diagnosed by the presence of one or more episodes of microangiopathic hemolytic anemia and thrombocytopenia defined on the basis of hematocrit (Ht)<30%, hemoglobin <10mg/dl, serum lactate dehydrogenase (LDH)>460U/L, undetectable haptoglobin, fragmented erythrocytes in the peripheral blood smear, and platelet count <150,000/µl, associated with acute renal failure. C3G was diagnosed by the presence of C3 deposits by immunofluorescence in the absence of immunogloblulins. The identification of dense deposits within the glomerular basement membrane by electron microscopy lead to further classification of the C3G as dense deposit disease (DDD). Our study also includes two R1210C pedigrees including 8 cases with AMD (2 carrying R1210C) and 3 healthy R1210C carriers. These pedigrees also include 11 healthy relatives who did not carry the R1210C mutation. AMD patients were recruited by the

Department of Ophthalmology, Clínica Universidad de Navarra, Pamplona, Spain. AMD was diagnosed by the presence of drusen and a chorioretinal macular atrophy involving central macula or signs related to CNV in at least one eye.

Genotyping and mutation screening. Genomic DNA was extracted from peripheral blood using standard procedures or from oral swabs using QIAcube (QIAGEN, Valencia, CA). DNA samples were genotyped for seven SNPs in four of the genes previously shown to be associated with AMD (CFH Ile62Val, CFH Tyr402His, CFH c.2237-543A>G, CFB Leu9His, CFB Arg32Gln/Trp, C3 Arg102Gly and ARMS2 Ala69Ser). The genotyping was performed using multiplex PCR and primer extension methodology (ABI Snapshot, Applied Byosistem, Foster City, CA) in a 3730 automated sequencer (Applied Byosistem, Foster City, CA). The fragments were analyzed with the Applied Biosystems GeneMapper Software v4.0. Exons of the *CFH, MCP, CFI, C3, CFB* and *THBD* genes were amplified from genomic DNA using primers derived from the intronic sequences as described (4-9). Automatic sequencing was performed in an ABI3730 sequencer using a dye terminator cycle sequencing kit (Applied Biosystems). The analysis of the $\Delta_{CFHR3\text{-}CFHR1}$ polymorphism and genomic rearrangements in the *CFH-CFHRs* region was by multiplex ligation-dependent probe amplification (MLPA) with the P236 A1 ARMD mix 1 (MRC-Holland, Amsterdam, Netherlands).

Purification of WT and mutant FHs. FH-WT, FH-R1210C and FH-S1129L-V1191I were purified to homogeneity from plasma of appropriate donors by affinity chromatography. Three affinity chromatography columns were used following the scheme depicted in Suppl. Fig. 4. Thirty mg of 214 moAb (anti-human FH, in-house) was coupled to a 5ml CNBr-activated Sepharose 4B column according to the manufacturer's instructions (GE Healthcare). Similarly, thirty mg of FH-402His moAb MBI-7 (anti-human FH-402His variant, in-house) was coupled to a 5ml CNBr-activated Sepharose 4B column. HiTrap Albumin and IgG depletion columns (GE Healthcare) were used to separate WT and

R1210C mutant FH. Bound FH to all columns was eluted with 0.1M Glycine/HCl pH 2.5 and immediately neutralised with 2M Tris pH 8. Aggregated material and minor contaminants were removed by gel filtration on Superdex 200 equilibrated in Hepes 10mM, NaCl 150 mM, pH7.4. Purity of the proteins was analyzed by SDS-PAGE under non-reducing and reducing conditions, and concentrations of all FHs were adjusted to exactly 1μM (Supplementary Figure 2).

Biosensor Analysis. All surface plasmon resonance analyses were carried out on a Biacore X100 (GE Healthcare). For the characterization of moAb binding to FH, approximately 50 RU of purified moAbs Ox24, MBI-6, MBI-7 or A229 were captured to a CM5 sensor chip using the Mouse Antibody capture Kit (GE Healthcare). The affinity of WT and mutant FH variants for each moAb was determined using a multi-cycle-kinetics method. Previously quantified FH samples were flowed at increasing concentrations in the presence of Hepes 10mM, NaCl 150mM, 0.005% tween-20, pH 7.4 for 150s or 300s, at a flow rate of 30 μl/min, and then allowed to decay for 1200s. The chip surface was regenerated with 10mM Glycine pH 1.5, followed by 100mM sodium acetate, NaCl 500 mM, pH 4.0. For each cycle, signal was double-referenced (data from a reference cell and blank injection subtracted) and all data evaluated using Biaevaluation software (version 4.1; GE Healthcare). Each FH injection was individually fitted and kinetics constants calculated using a one-to-one binding interaction model. Although the interaction between the FH-R1210C mutant and moAb A229 was also decreased compared to other FHs, it could not be fitted to a simple binding interaction model to provided accurate kinetic constants.

To test the decay acceleration activity of the FH variants we used a low density C3b amino coupled CM5 sensor chip (450 RU) to eliminate the risk of FH N- and C-terminal regions interacting simultaneously with two different C3b molecules. To form the AP C3 convertase, FB (1μM) and FD (40nM) in HEPES 10mM pH 7.4, NaCl 150mM, $MgCl_2$ 5mM and 0.005% tween-20, were flowed until 50 additional RUs were generated. FH

samples were then flowed at 70 nM during 500s at a flow rate of 10 µl/min and decay accelerating activity was monitored. Spontaneous decay was monitored by flowing running buffer instead of FH. The C3b surface was regenerated with 100mM sodium acetate pH 4.0, NaCl 500 mM. Three independent decay experiments with identical results were performed for each FH variant. All signals were double-referenced (data from a reference cell and blank injection subtracted).

References for Supplementary Methods

1. Gorin MB. Genetic insights into age-related macular degeneration: Controversies addressing risk, causality, and therapeutics. *Mol Aspects Med.* 2012.
2. Noris M, and Remuzzi G. Atypical hemolytic-uremic syndrome. *N Engl J Med.* 2009;361(17):1676-87.
3. Xiao X, Pickering MC, and Smith RJ. C3 glomerulopathy: the genetic and clinical findings in dense deposit disease and C3 glomerulonephritis. *Seminars in Thrombosis and Hemostasis.* 2014;40(4):465-71.
4. Delvaeye M, et al. Thrombomodulin mutations in atypical hemolytic-uremic syndrome. *N Engl J Med.* 2009;361(4):345-57.
5. Fremeaux-Bacchi V, et al. Complement factor I: a susceptibility gene for atypical haemolytic uraemic syndrome. *J. Med. Genet.* 2004;41(6):e84.
6. Fremeaux-Bacchi V, et al. Mutations in complement C3 predispose to development of atypical hemolytic uremic syndrome. *Blood.* 2008;112(13):4948-52.
7. Goicoechea de Jorge E, et al. Gain-of-function mutations in complement factor B are associated with atypical hemolytic uremic syndrome. *Proc Natl Acad Sci U S A.* 2007;104(1):240-5.

8. Perez-Caballero D, et al. Clustering of Missense Mutations in the C-Terminal Region of Factor H in Atypical Hemolytic Uremic Syndrome. *Am. J. Human Genet.* 2001;68(2):478-84.

9. Richards A, et al. Mutations in human complement regulator, membrane cofactor protein (CD46), predispose to development of familial hemolytic uremic syndrome. *Proc Natl Acad Sci U S A.* 2003;100(22):12966-71.

SUPPLEMENTARY FIGURES

Supplementary Figure 1

	ID (PED #)	AMD Risk						aHUS Risk		
		CFH V62I	*CFH* Y402H	*CFB* L9H	*CFB* R32Q/W	*ARMS2* A69S	*CFHR1* A/B/Del	Add. Mut.	*CFH*	*MCP*
aHUS cases and relatives	F104-270 (H024)	G/G	T/C	T/T	R/Q	G/G	A/A	1 (*MCP*)	NO	NO
	F106 (H024)	G/G	T/T	T/A	R/R	G/G	B/Del	2 (*MCP*)	NO	NO
	F108 (H024)	G/G	T/T	T/A	R/R	G/G	B/Del	2 (*MCP*)	NO	NO
	S006-396 (H069)	G/G	T/T	T/T	W/W	G/G	B/Del	NO	HET	NO
	S013-397 (H069)	G/G	T/T	T/T	Q/W	G/G	B/Del	NO	HET	NO
	R018-358 (H020)	G/G	T/C	T/T	R/W	G/G	A/B	NO	HET	NO
	R016-214 (H020)	G/G	T/C	T/T	Q/W	G/G	A/B	NO	NO	HET
	R026-416 (H020)	G/G	T/C	T/T	R/R	G/T	A/B	NO	NO	HET
	R028-432 (H020)	G/A	T/T	T/T	R/R	G/T	B/B	NO	NO	NO
	R017-361 (H020)	G/A	T/T	T/T	R/W	G/G	B/B	NO	NO	NO
	R021-360 (H020)	G/A	T/T	T/T	R/W	G/G	B/B	NO	NO	NO
	R025-426 (H020)	G/G	T/C	T/T	Q/W	G/G	A/B	NO	NO	NO
	R639-639 (H020)	G/A	T/T	T/T	R/R	G/G	B/B	NO	NO	NO
	HUS300 (H300)	G/G	T/T	T/T	R/W	G/G	B/B	NO	HOM	NO
	C04 (H300)	G/G	T/T	T/T	R/Q	G/G	B/B	NO	HOM	NO
	C21 (H300)	G/G	T/T	T/T	R/W	G/T	B/B	NO	HOM	NO
	MC (H300)	G/G	T/T	T/T	R/W	G/T	B/B	NO	HOM	NO
	S198-206-673	G/G	T/T	T/T	R/W	G/G	B/Del	NO	HET	HOM
	S197-090-659	G/G	T/C	T/T	R/R	G/T	A/A	NO	NO	HOM
	S196-177-626	G/G	T/T	T/T	R/R	T/T	B/Del	NO	HET	HET
	881-1632	G/G	T/C	T/T	R/R	G/G	A/B	NO	HET	HET
	350-978	G/G	T/T	T/T	R/R	G/G	B/B	1(MCP); 1(CFI)	HET	HET
	856-1591	G/G	T/T	T/T	R/W	G/G	B/B	NO	HOM	HOM
	HUS29	G/G	T/C	T/T	R/R	G/G	A/A	1 (*CFH*)	NO	HOM
	S223-242-819	G/G	T/T	T/T	R/R	G/G	B/Del	NO	HOM	HOM
C3G	1101 (DDD447)	G/A	T/T	T/T	R/R	G/G	B/B	NO	NO	HOM
	1234 (DDD447)	G/A	T/T	T/T	R/R	G/G	B/B	NO	NO	HOM
AMD cases and relatives	1 (F1)	G/G	T/C	T/A	R/R	G/T	A/Del	NO	NO	NO
	2 (F1)	G/G	C/C	T/T	R/Q	G/T	A/A	NO	NO	NO
	3 (F1)	G/A	T/T	T/T	R/R	G/T	B/B	NO	NO	HET
	4 (F1)	G/G	C/C	T/T	R/R	G/T	A/A	NO	NO	HET
	5 (F1)	G/A	T/C	T/A	R/R	G/T	A/B	NO	NO	NO
	6 (F1)	G/G	T/C	T/T	R/R	G/T	A/A	NO	NO	NO
	7 (F1)	G/G	T/C	T/T	R/R	G/T	A/A	NO	NO	NO
	8 (F1)	G/G	T/T	T/T	R/W	G/T	A/Del	NO	NO	NO
	9 (F1)	G/G	T/T	T/A	R/R	T/T	A/Del	NO	NO	NO
	10 (F1)	G/G	T/C	T/T	R/Q	G/T	A/A	NO	NO	NO
	11 (F1)	G/G	T/C	T/T	R/Q	G/G	A/Del	NO	NO	NO
	12 (F1)	G/G	T/T	T/T	R/R	G/G	A/B	NO	HET	HET
	13 (F1)	G/G	C/C	T/T	R/Q	G/T	A/A	NO	NO	NO
	14 (F1)	G/G	T/T	T/T	R/W	G/T	Del/Del	NO	NO	NO
	15 (F1)	G/G	T/T	T/A	R/R	G/G	Del/Del	NO	NO	NO
	17 (F1)	G/G	n/a	T/T	R/R	G/G	A/B	NO	NO	NO
	097IA (F3)	G/G	T/C	T/T	R/R	G/G	A/A	NO	NO	NO
	1 (F3)	G/G	T/C	T/T	R/W	G/G	A/A	NO	NO	NO
	2 (F3)	G/G	T/C	T/T	R/R	G/T	A/A	NO	NO	HET
	3 (F3)	G/G	C/C	T/T	R/R	G/T	A/A	NO	NO	HET
	4 (F3)	G/G	T/C	T/T	R/R	T/T	A/A	NO	NO	HET
	5 (F3)	G/G	T/T	T/T	R/R	G/G	A/A	NO	NO	HET

Genotypes used in the calculation of the aHUS and AMD overall risks.

Supplementary Figure 2

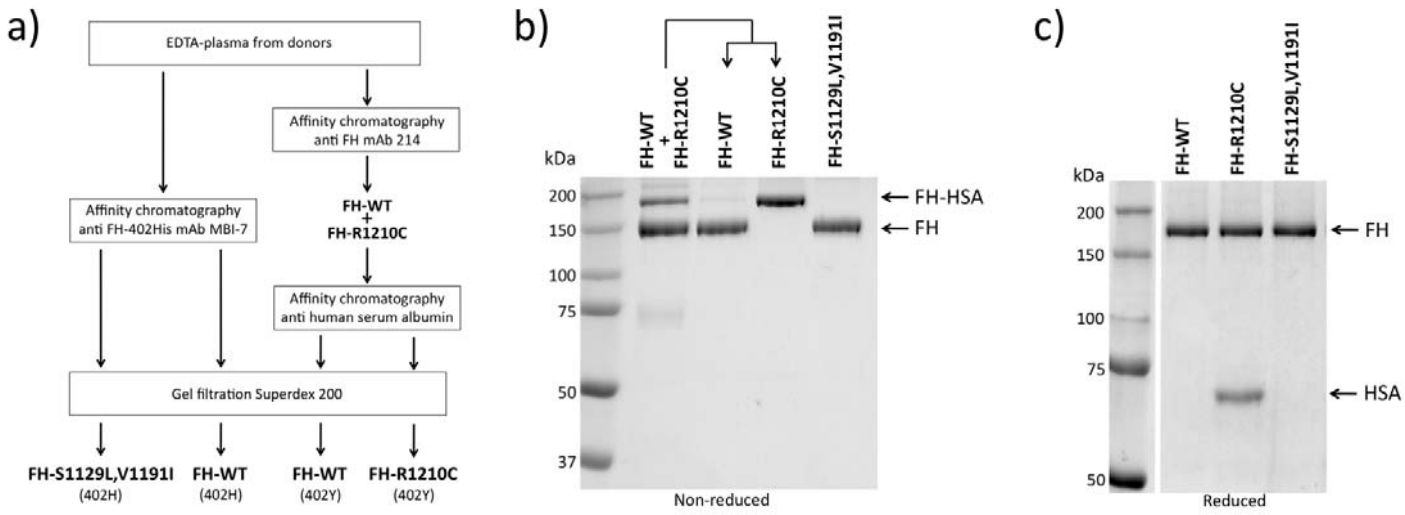

Purification of WT and mutant FH proteins.

FH-R1210C, FH-WT-402H, FH-WT-402Y and FH-S1129L-V1191I were purified to homogeneity from appropriate donors as indicated in (a). Purity of the proteins was analyzed by SDS-PAGE under non-reducing (b) and reducing conditions (c) and concentrations of the three FHs were adjusted to exactly 1μM. Notice that the FH-R1210C mutant runs as a high molecular weight band under non-reducing conditions (FH-HSA complex). This complex separates into FH and HSA under reducing conditions. HSA, human serum albumin.

Supplementary Figure 3

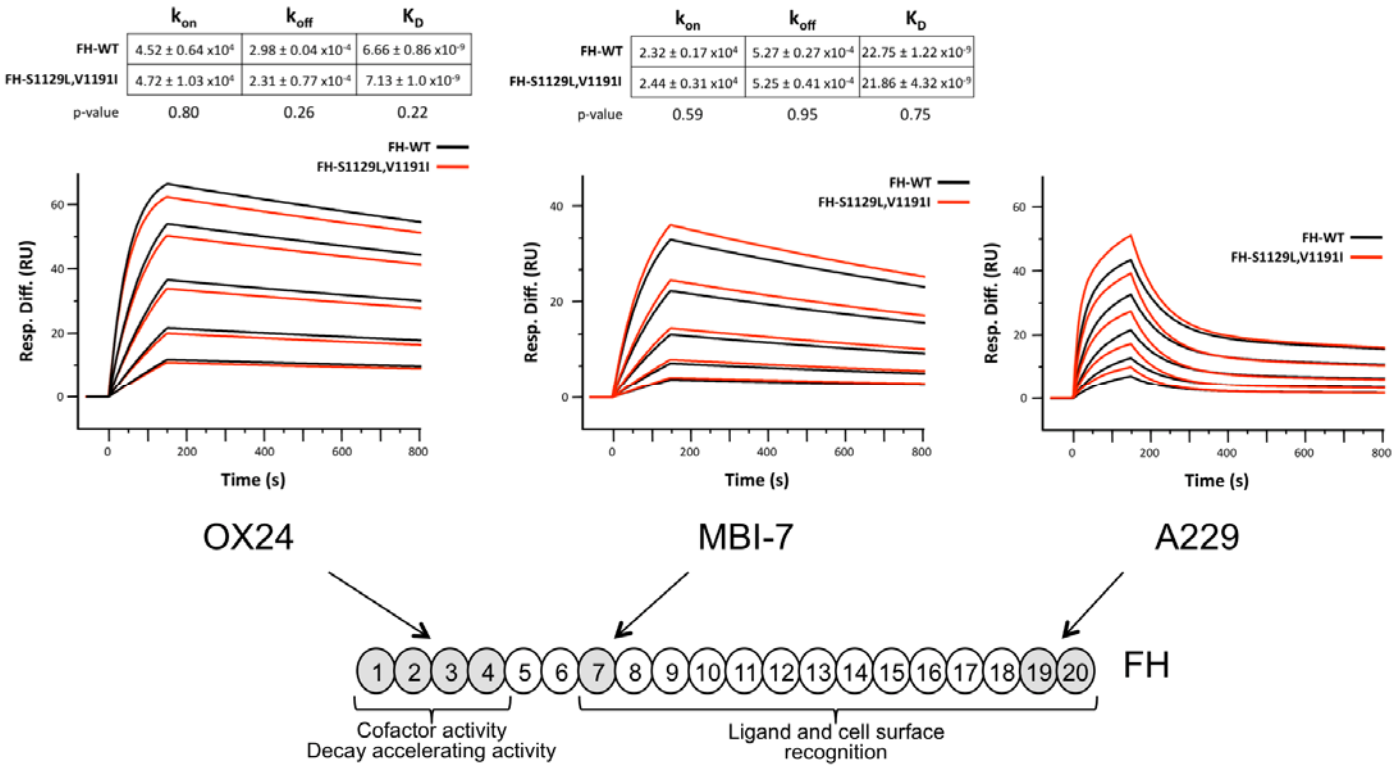

Analysis of accessibility to functional domains in the aHUS-specific FH-S1129L,V1191I mutant.

Panels depict the binding of purified FH-WT (black) and FH-S1129L,V1191I (red) (both 402H) to captured Ox24, MBI-7 and A229 moAbs at increasing concentrations (800nM, 400nM, 200nM, 100nM and 50nM). Sensograms for Ox24 and MBI-7 moAbs show the fitted curves and kinetic constants calculated using a one-to-one interaction model. Values are the means of three independent experiments (Online Methods). In contrast to moAbs OX24 and MBI-7, the binding of FH-WT and FH-S1129L,V1191I to moAb A229 only fitted a heterogeneous ligand model, which was defined by multiple kinetic constants. Note that, as expected, no significant differences were observed in the binding of FH-WT and FH-S1129L,V1191I to the three moAbs.